Current Biology *16*, 2073–2079, October 24, 2006 ©2006 Elsevier Ltd All rights reserved DOI 10.1016/j.cub.2006.08.085

Report

CRACM1 Multimers Form the Ion-Selective Pore of the CRAC Channel

Monika Vig,[2,4] Andreas Beck,[1,4] James M. Billingsley,[2,4] Annette Lis,[1] Suhel Parvez,[1] Christine Peinelt,[1] Dana L. Koomoa,[1] Jonathan Soboloff,[3] Donald L. Gill,[3] Andrea Fleig,[1] Jean-Pierre Kinet,[2,*] and Reinhold Penner[1,*]

[1] Center for Biomedical Research at The Queen's Medical Center and
John A. Burns School of Medicine
University of Hawaii, Honolulu
Honolulu, Hawaii 96813
[2] Department of Pathology
Beth Israel Deaconess Medical Center and
Harvard Medical School
Boston, Massachusetts 02215
[3] Department of Biochemistry and Molecular Biology
School of Medicine
University of Maryland
Baltimore, Maryland 21201

Summary

Receptor-mediated Ca^{2+} release from the endoplasmic reticulum (ER) is often followed by Ca^{2+} entry through Ca^{2+}-release-activated Ca^{2+} (CRAC) channels in the plasma membrane [1–5]. RNAi screens have identified STIM1 as the putative ER Ca^{2+} sensor [6–8] and CRACM1 (Orai1; [9–11]) as the putative store-operated Ca^{2+} channel. Overexpression of both proteins is required to reconstitute CRAC currents (I_{CRAC}; [11–14]). We show here that CRACM1 forms multimeric assemblies that bind STIM1 and that acidic residues in the transmembrane (TM) and extracellular domains of CRACM1 contribute to the ionic selectivity of the CRAC-channel pore. Replacement of the conserved glutamate in position 106 of the first TM domain of CRACM1 with glutamine (E106Q) acts as a dominant-negative protein, and substitution with aspartate (E106D) enhances Na^+, Ba^{2+}, and Sr^{2+} permeation relative to Ca^{2+}. Mutating E190Q in TM3 also affects channel selectivity, suggesting that glutamate residues in both TM1 and TM3 face the lumen of the pore. Furthermore, mutating a putative Ca^{2+} binding site in the first extracellular loop of CRACM1 (D110/112A) enhances monovalent cation permeation, suggesting that these residues too contribute to the coordination of Ca^{2+} ions to the pore. Our data provide unequivocal evidence that CRACM1 multimers form the Ca^{2+}-selective CRAC-channel pore.

*Correspondence: jkinet@bidmc.harvard.edu (J.-P.K.), rpenner@hawaii.edu (R.P.)
[4] These authors contributed equally to this work.

Results and Discussion

CRACM1 Associates with Itself to Form the CRAC-Channel Complex

Both STIM1 and CRACM1 are crucial elements of store-operated Ca^{2+} entry. The STIM1 protein, containing a single membrane-spanning domain, likely senses endoplasmic reticulum (ER) Ca^{2+} levels by virtue of its luminal-facing EF-hand domain [6–8, 15] and accumulates into ER puncta close to the plasma membrane in response to store depletion [6–8, 15, 16], whereas CRACM1 is proposed as the pore-forming unit of the channel itself because, reconstituted with STIM1, it results in massive Ca^{2+}-release-activated Ca^{2+} (CRAC) channel activation in response to store depletion [11–14]. CRACM1 is a relatively small protein (301 amino acids), predicted to contain four transmembrane domains with N and C termini facing the cytosol [9, 10]. Because many ion channels multimerize to form a functional ion pore, we tested CRACM1's propensity to multimerize by co-overexpressing two differently tagged versions of the protein in HEK293 cells and performing reciprocal coimmunoprecipitation experiments followed by immunoblotting with the relevant anti-tag antibodies. Figure 1A illustrates that each tagged version of CRACM1 coimmunoprecipitates with the other, indicating that CRACM1 indeed multimerizes with itself. Because STIM1 moves to the plasma membrane after store depletion, it might interact with CRACM1. We tested this with differently tagged CRACM1 and STIM1 cooverexpressed in HEK293 cells and subjected to reciprocal immunoprecipitation followed by immunoblotting with the relevant anti-tag antibodies. As shown in Figure 1B, both proteins coimmunoprecipitated, suggesting that they bind to each other.

CRAC channels are highly selective for Ca^{2+} ions [1, 2], with limited permeation of Ba^{2+} or Sr^{2+} and largely impermeant to monovalent cations such as Na^+, K^+, or Cs^+ [1, 2, 17]. Removal of extracellular Ca^{2+}, while maintaining 1–2 mM Mg^{2+}, essentially abolishes CRAC inward currents. However, upon removal of all divalent cations, I_{CRAC} becomes a nonselective current that conducts monovalent ions [2]. Previous work on voltage-gated Ca^{2+} channels has elucidated the structural basis for their Ca^{2+} selectivity and identified transmembrane glutamate residues in the S5-S6 linker regions as crucial structural features of the ion-conducting pore [18, 19]. We analyzed the primary sequence of CRACM1 and identified glutamate residues E106 in TM1 and E190 in TM3, both of which are highly conserved for CRACM1 and its homologs CRACM2 and CRACM3 (Orai2 and Orai3) as well as across several species (see Figure 1C). In addition, the first extracellular loop, linking TM1 and TM2 domains, contains several negatively charged aspartate residues (D110, D112, and D114) that could potentially be part of a Ca^{2+} binding site. We constructed several CRACM1 mutants in which we modified these residues to test for their possible involvement in forming

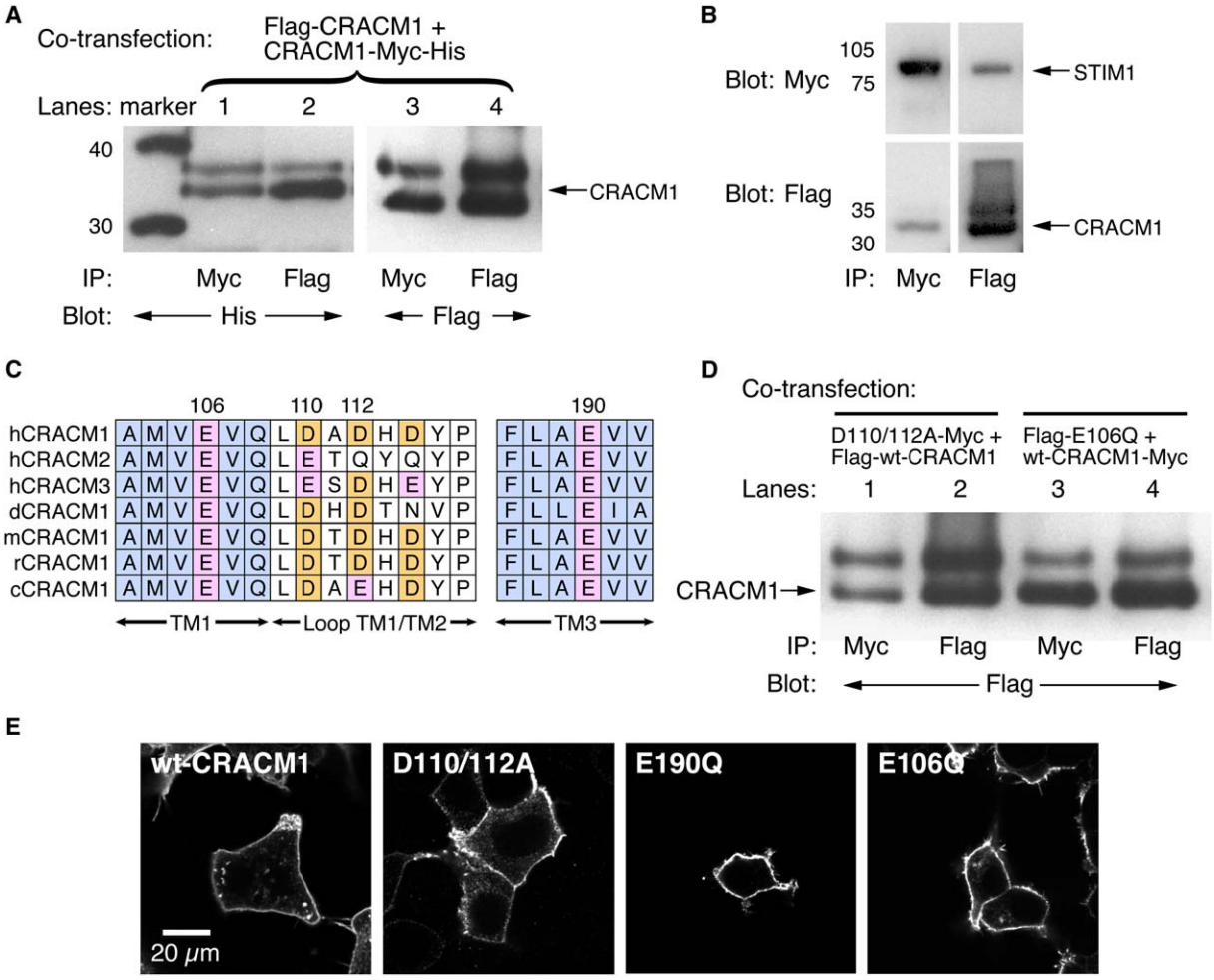

Figure 1. CRACM1 Multimerizes with Itself to Form the CRAC Channel

(A) Coimmunoprecipitation (co-IP) of CRACM1 from HEK293 cells cotransfected with Flag-CRACM1 and CRACM1-Myc-His. Lane 2 shows that Flag-CRACM1 can co-IP CRACM1-Myc-His. Lane 3 shows the reverse co-IP, and lanes 1 and 4 show the control IPs.

(B) Co-IP of Flag-CRACM1 and STIM1-Myc-His, cotransfected in HEK293 cells. Whole-cell lysates were immunoprecipitated with either myc antibody (first lane) or Flag antibody (second lane) and blotted with either myc antibody (upper panels) or Flag antibody (lower panels). The same experiment was done with the E106Q, D110/112A, and E190Q CRACM1 mutants. These mutations did not impair CRACM1-STIM1 coassociation (data not shown).

(C) Sequence alignment of human CRACM1, CRACM2, and CRACM3 as well as CRACM1 from various species (*Drosophila*, mouse, rat, and chicken), highlighting the acidic residues (residue numbers pertain to the human sequence of CRACM1).

(D) Co-IP of D110/112A-CRACM1 and E106Q-CRACM1 mutant with the wild-type CRACM1. Lane 1 shows that D110/112A-CRACM1-Myc-His can co-IP Flag-CRACM1, and lane 3 shows that CRACM1-Myc-His can co-IP Flag-E106Q-CRACM1. Lanes 2 and 4 show the controls.

(E) Confocal images of HEK293 cells transfected with Flag-CRACM1, D110/112A-CRACM1-Myc-His, Flag-E190Q-CRACM1, and Flag-E106Q-CRACM1 and stained with myc or Flag antibodies, respectively, to show cellular localization of the mutants.

the pore of the CRAC channel and conferring the high specificity for Ca^{2+}. Coimmunoprecipitation confirmed that these mutant proteins retain the capacity to multimerize (Figure 1D), and confocal microscopy revealed proper targeting to the plasma membrane (Figure 1E). We then overexpressed these mutant proteins in HEK293 cells that stably overexpress STIM1 and analyzed them electrophysiologically by whole-cell patch-clamp recordings in which we induced CRAC currents by IP_3-mediated Ca^{2+} store depletion.

Transmembrane Domains 1 and 3 of CRACM1 Form the Ca^{2+}-Selective Ion-Channel Pore

We first generated a point mutant of CRACM1 in which the glutamate in TM1 at position 106 was changed to a glutamine residue (E106Q). When transfected into STIM1-overexpressing HEK293 cells, this mutant inhibited thapsigargin-induced Ca^{2+} influx in fura-2 fluorescence measurements (data not shown), and patch-clamp recordings confirmed that this mutant not only failed to produce large CRAC currents as did the wild-type CRACM1 (Figures 2A and 2B), but also caused a complete suppression of the small endogenous CRAC currents (~0.5 pA/pF) typically seen in STIM1-overexpressing cells or untransfected HEK293 cells [10, 13]. Even exposure to divalent-free solution, which in wild-type CRACM1 generates large monovalent currents [13], failed to produce sizeable inward currents (Figure 2A). Given that the mutation did not affect the capacity of CRACM1 to multimerize (Figure 1D) or its transport

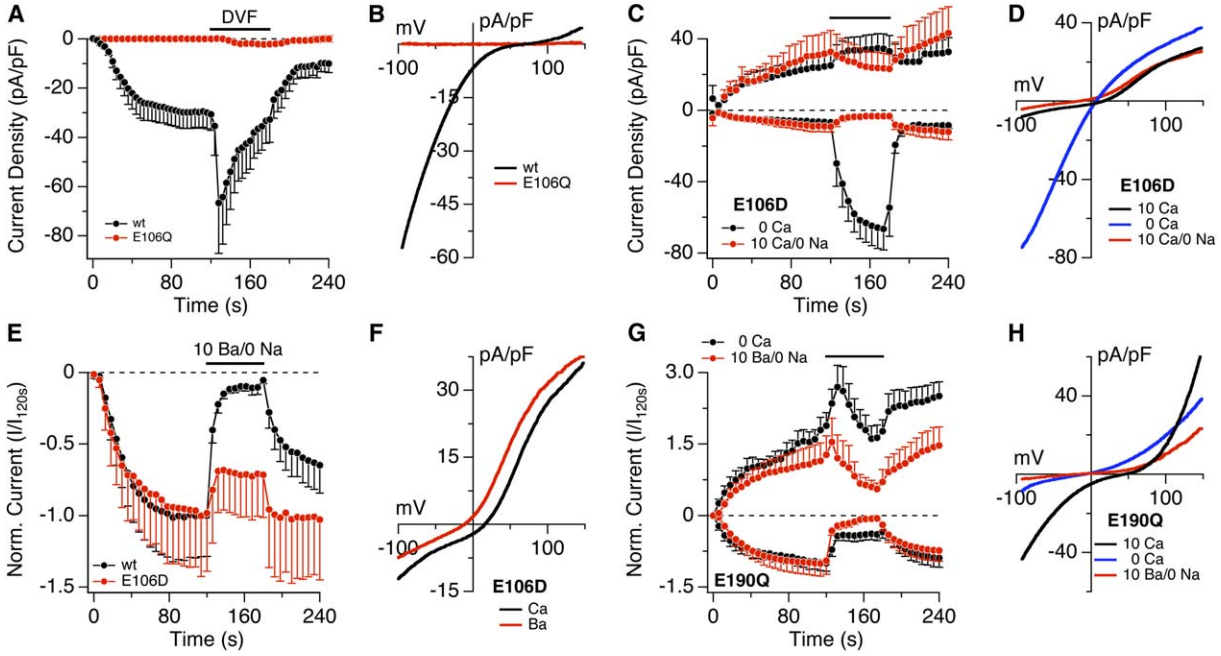

Figure 2. The E106 Residue Is Part of the Selectivity Filter of CRACM1

(A) Normalized average time course of IP_3-induced (20 μM) CRAC currents measured in HEK293 cells co-overexpressing STIM1 and wild-type CRACM1 (black circles, n = 14) and E106Q mutation (red circles, n = 9). Currents of individual cells were measured at −80 mV, normalized by cell capacitance, averaged and plotted versus time (± SEM). Cytosolic calcium was clamped to near zero with 20 mM BAPTA. The bar indicates application of divalent-free (DVF) solution.

(B) Average current-voltage (I/V) relationships of CRAC currents extracted from representative HEK293 cells shown in (A) at 120 s into the experiment. Data represent leak-subtracted currents evoked by 50 ms voltage ramps from −100 to +150 mV, normalized to cell capacitance (pF). Traces correspond to STIM1 + wild-type CRACM1 (wild-type, n = 12) or STIM1 + E106Q mutant (n = 6).

(C) Normalized average time course of IP_3-induced (20 μM) currents at −80 and +130 mV produced by the E106D mutant. Cells were exposed to nominally Ca^{2+}-free external solution (black circles, n = 6) or Na^+-free solution (red circles, n = 6) for the time indicated by the black bar. Currents were analyzed as in (A).

(D) Average I/V traces of the E106D mutant extracted at 120 s (black trace, n = 6) and at the end of the application of Ca^{2+}-free (blue trace, n = 6) or Na^+-free (red trace, n = 6) solutions (same cells as in [C]). Data analysis was as in (B).

(E) Normalized average time course of CRAC currents in HEK293 cells expressing STIM1 and wild-type CRACM1 (black circles, n = 9) or E106D mutant (red circles, n = 7). Analysis was as in (A). Cells were superfused with external solution containing 10 mM Ba^{2+} (and 0 Ca^{2+}) at the time indicated by the black bar. Note that cells were superfused with Ba^{2+} in the absence of extracellular Na^+ (replaced by TEA^+) to avoid Na^+ current contamination.

(F) Average I/V data traces of currents extracted from representative HEK293 cells expressing the E106D mutant shown in (E), before (120 s, n = 4) and at the end (180 s, n = 4) of Ba^{2+} application. Analysis was as in (B).

(G) Normalized average time course of IP_3-induced (20 μM) currents at −80 and +130 mV produced by the E190Q mutant. Cells were exposed to nominally Ca^{2+}-free external solution (black circles, n = 7) or Na^+-free solution, where Ca^{2+} was substituted with Ba^{2+} (red circles, n = 8) for the time indicated by the bar. Currents were analyzed as in (A).

(H) Average I/V traces of the E190Q mutant extracted at 120 s (black trace, n = 8) and at the end of the application of 10 mM Ba^{2+} (red trace, n = 8) or Ca^{2+}-free solutions (blue trace, n = 7; same cells as in [G]). Data analysis was as in (B).

to the plasma membrane (Figure 1E), this result suggests that the E106Q mutant acts as a dominant-negative protein that can form normal CRACM1 complexes and even coassemble with endogenous CRACM1, but is not able to provide a pore that would allow permeation of either Ca^{2+} or Na^+ ions.

We therefore made a charge-conserving mutation by converting the glutamate into an aspartate residue (E106D). This mutant exhibited membrane currents that activated similarly as wild-type CRACM1 after IP_3-mediated store depletion, but were smaller on average (−8 ± 1 pA/pF, n = 12 versus −30 ± 6 pA/pF, n = 14; cf. Figures 2A and 2C). The selectivity of these mutated CRACM1 channels also differed markedly from that of wild-type CRACM1, converting the typically inwardly rectifying current-voltage relationship into outwardly rectifying and shifting its reversal potential from far positive voltages toward 0 mV (cf. Figures 2B and 2D), suggesting a significant loss in Ca^{2+} selectivity. The prominent outward currents developed with exactly the same time course as the inward current and are therefore likely carried by the major intracellular cation Cs^+ flowing through CRAC channels. Upon removal of extracellular Ca^{2+}, the current reversed to inward rectification as a result of a massive increase of inward current and a slight increase in outward current. It should be noted that these effects were obtained by a simple removal of Ca^{2+} while the presence of 2 mM Mg^{2+} was maintained, which normally prevents any monovalent inward or outward currents through wild-type CRACM1 channels. The large increase in inward current upon removal of Ca^{2+} suggests that the channel still conducts Ca^{2+} ions inwardly when Ca^{2+} ions are present and precludes massive Na^+ flux. We confirmed this by

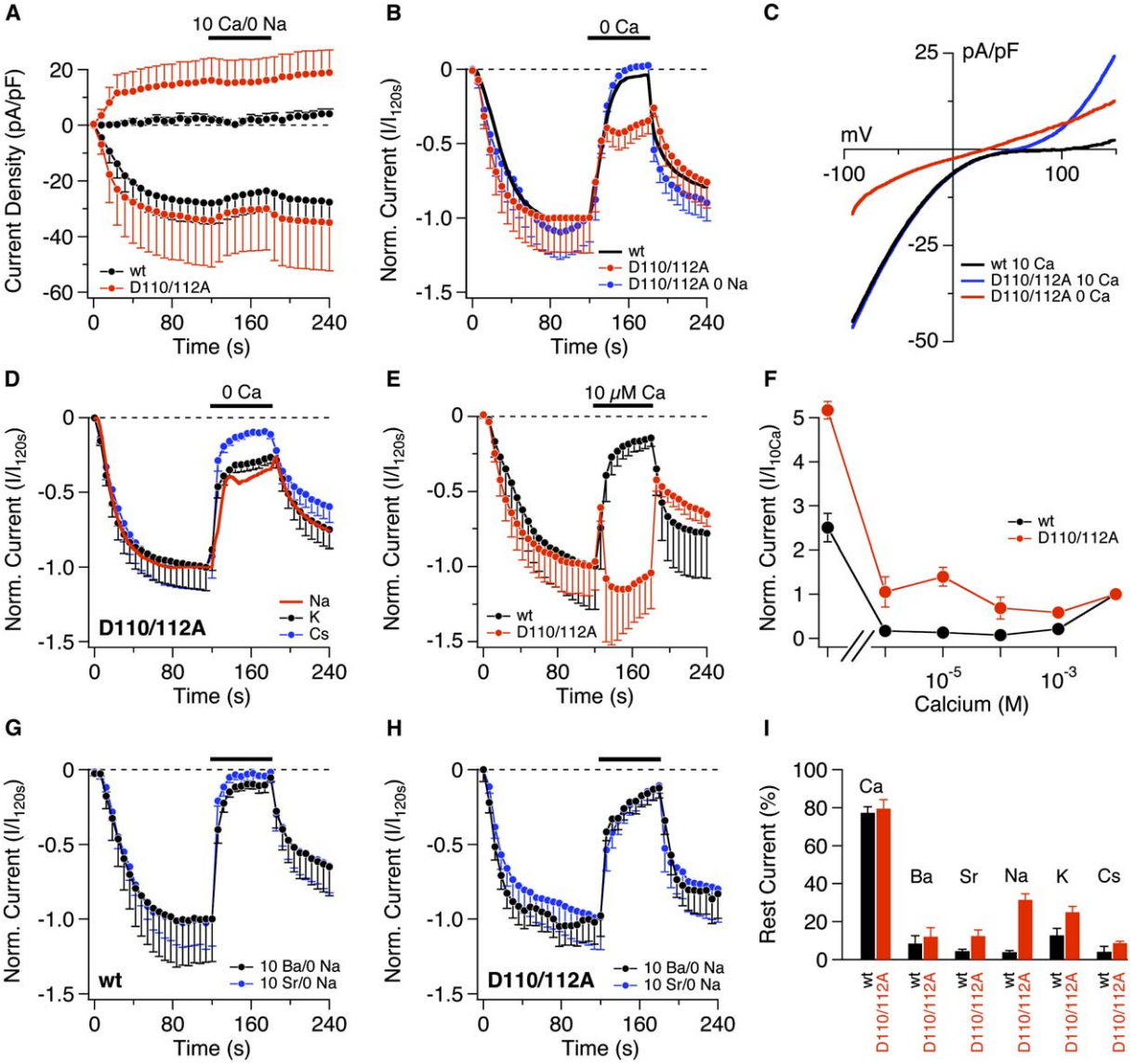

Figure 3. A Putative Extracellular Ca^{2+} Binding Site Contributes to Selectivity of CRACM1

(A) Normalized average time course of IP_3-induced (20 μM) CRAC currents measured in HEK293 cells coexpressing STIM1 with either wild-type CRACM1 (black circles, n = 12) or the D110/112A mutant of CRACM1 (red circles, n =11). Currents of individual cells were measured at −80 mV and +130 mV, normalized by cell capacitance, averaged, and plotted versus time (± SEM). Cytosolic calcium was clamped to near zero with 20 mM BAPTA. The black bar indicates application of an external solution containing 10 mM Ca^{2+} with Na^+ replaced by TEA^+.

(B) Average time course of IP_3-induced (20 μM) currents produced by wild-type CRACM1 (black trace, same data as in Figure 2A) or D110/112A mutant. Currents were normalized to unity at 120 s (I/I_{120s}). Cells expressing the D110/112A mutant were superfused with nominally Ca^{2+}-free external solution in the presence (130 mM, n = 13) or absence of Na^+ (TEA^+ substitution, n = 5). Perfusion time is indicated by the black bar. Currents were analyzed as in (A).

(C) Average I/V relationships of CRAC currents extracted from representative HEK293 cells shown in (A) and (B). Data represent average leak-subtracted currents evoked by 50 ms voltage ramps from −100 to +150 mV and normalized to cell capacitance (pF). Traces show wild-type CRACM1-expressing cells (black trace, n = 10; scaled by 1.7 to fit inward-current size of D110/112A mutant) at the end of application of a Na^+-free solution containing 10 mM Ca^{2+} (180 s) and D110/112A mutants extracted before (at 120 s, blue trace, n = 11) or during application of nominally Ca^{2+}-free solution containing normal Na^+ (red trace, n = 11).

(D) Normalized average time course (I/I_{120s}) of IP_3-induced (20 μM) currents produced by the D110/112A mutant in cells superfused with nominally Ca^{2+}-free solution containing Na^+ (red line, same data as in [B]), K^+ (black circles, n = 12) or Cs^+ (blue circles, n = 9). Application time is indicated by the black bar. Currents were analyzed as in (A).

(E) Normalized average time course (I/I_{120s}) of IP_3-induced (20 μM) currents produced by wild-type CRACM1 (black circles, n = 8) or D110/112A mutant (red circles, n = 8). Cells were superfused with nominally divalent-free external solution supplemented with 10 μM Ca^{2+} as indicated by the black bar. Currents were analyzed as in (A).

(F) Anomalous mole-fraction effect of wild-type CRACM1 (black circles, n = 5–14) or D110/112A mutant (red circles, n = 5–8). Current sizes measured at different Ca^{2+} concentrations were set in relation to current amplitudes obtained with 10 mM Ca^{2+}, averaged and plotted against increasing extracellular Ca^{2+} concentrations.

(G) Normalized average time course (I/I_{120s}) of IP_3-induced (20 μM) currents produced by wild-type CRACM1 in cells superfused with an external solution where 10 mM Ca^{2+} was equimolarly substituted with Ba^{2+} (black circles, n = 9) or Sr^{2+} (blue circles, n = 7) in the absence of Na^+ (replaced by TEA^+ to avoid Na^+ current contamination). Currents were analyzed as in (A).

experiments in which we maintained extracellular Ca^{2+} at 10 mM and replaced extracellular Na^+ by nonpermeant TEA^+. This caused a reduction in inward current by ~50% (Figures 2C and 2D), where the remaining inward current is carried by Ca^{2+} ions and the outward current by the predominant intracellular Cs^+ ions.

Additional ion-substitution experiments confirmed that the modified selectivity of this mutant is not limited to monovalent cations, but also affects the relative permeability of Ba^{2+} ions. Figures 2E and 2F illustrate that the equimolar substitution of Ca^{2+} by Ba^{2+} causes only a small decrease in inward current, a result that is in marked contrast to the wild-type CRACM1 channel, where the same ion substitution reduces inward currents by ~90%. Thus, the E106D mutant has a significantly increased Ba^{2+} permeation compared to the wild-type. Together, these results suggest that the E106 residue is a crucial structural element that confers the CRAC channel's high Ca^{2+} selectivity und unequivocally demonstrates that CRACM1 indeed represents the pore-forming subunit of the CRAC channel. In addition, it seems plausible to suggest that the E106 residues of several CRACM1 subunits may form a concentric ring of negative charges lining the channel pore to form the selectivity filter and favor Ca^{2+} ions over all other cations. However, in voltage-gated Ca^{2+} channels, it is found that four glutamate residues in equivalent positions of each of the four repeats I–IV interact to allow the binding of two Ca^{2+} ions in close proximity [19]. Hence, the CRACM1 channel may contain additional residues that contribute to Ca^{2+} binding and selectivity.

Sequence analysis reveals in TM3 another acidic and negatively charged residue (E190) that is equally well conserved across CRACM proteins. We constructed a mutant in which we replaced this glutamate by a glutamine residue (E190Q mutation). When transfected into STIM1-expressing HEK293 cells, we found that this mutant activated normally after IP_3-induced store depletion and generated inward currents that were primarily carried by Ca^{2+}, because removal of extracellular Ca^{2+} (while maintaining 2 mM Mg^{2+}) reduced inward currents by about 70% (Figure 2G). The remaining Na^+ current is larger than in wild-type CRACM1, suggesting reduced selectivity for Ca^{2+} over Na^+. However, in marked contrast to the E106D mutant, inward currents did not increase. Interestingly, the outward current through the E190Q mutant was more prominent and linear than that of the E106D mutant (Figure 2H), suggesting that monovalent outward permeation of Cs^+ is significantly enhanced in this mutant. Finally, we tested the E190Q mutant for Ba^{2+} permeability, which is very low in wild-type CRACM1, but significantly increased in the E106D mutant. Substitution of Ca^{2+} by Ba^{2+} resulted in almost complete abolition of inward current with only 5% of inward current remaining under Ba^{2+} (Figure 2G), suggesting that the E190Q mutant retains high Ca^{2+} selectivity over Ba^{2+} similar to wild-type CRACM1.

Together, these results suggest that both glutamates in position 106 in TM1 and position 190 in TM3 participate in shaping the selectivity of the CRAC channel. It is therefore reasonable to conclude that both likely face the luminal side of the aqueous pore and jointly provide the necessary constraints that impose the exquisite Ca^{2+} selectivity of the channel.

The First Extracellular Loop of CRACM1 Contributes to the Pore Selectivity

Adjacent to the critical E106 residue, in the first extracellular loop of CRACM1, there are three closely spaced aspartate residues (D110/112/114) that may participate in coordinating the binding of Ca^{2+} at the outer mouth of the channel. We generated a double mutant in this region by changing the most conserved negatively charged aspartate residues at positions 110 and 112 into alanines (D110/112A mutation). The predominant plasma-membrane localization of this mutant and its multimerization potential were comparable to those of wild-type CRACM1 (Figure 1D and 1E). The CRAC currents generated by the D110/112A mutant activated with a similar time course as those produced by the wild-type channel (Figure 3A). The inward currents of both constructs at −80 mV also were quite similar; however, the mutant showed a distinctive and much larger outward current at +130 mV than the wild-type channel. The current-voltage relationships of the wild-type and mutant constructs illustrate these features in more detail (Figure 3C). Thus, at negative voltages, both constructs exhibit similar inwardly rectifying currents, whereas at voltages more positive than +80 mV, the D110/112A mutant passes a significantly larger amount of outward current. Figure 3A also demonstrates that the inward currents of both wild-type and mutant channels remained largely unaffected when extracellular Na^+ was removed by replacing it with TEA^+ and maintaining 10 mM Ca^{2+} as the only charge carrier. This suggests that both channel constructs retain high selectivity for Ca^{2+} over Na^+ influx when 10 mM Ca^{2+} is present extracellularly.

However, because outward movement of monovalent cations was enhanced in the D110/112A mutant, we tested whether monovalent inward currents might be enhanced at low extracellular Ca^{2+}. We assessed this by ion-substitution experiments in which we removed extracellular Ca^{2+}. When Ca^{2+} is removed, while 130 mM Na^+ and 2 mM Mg^{2+} are retained, the wild-type CRAC current is essentially abolished (Figure 3B), demonstrating that the remaining Mg^{2+} completely prevents monovalent Na^+ permeation. In contrast, the inhibition of the inward current by the D110/112A mutant is not as complete, suggesting that the absence of Ca^{2+} allows for more Na^+ permeation than in the wild-type. The

(H) Normalized average time course (I/I_{120s}) of IP_3-induced (20 μM) currents produced by the D110/112A mutant in cells superfused with an external solution where 10 mM Ca^{2+} was substituted equimolarly with Ba^{2+} (black circles, n = 7) or Sr^{2+} (blue circles, n = 7) in the absence of Na^+ (replaced by TEA^+ to avoid Na^+ current contamination). Currents were analyzed as in (A).

(I) Permeation profile of wild-type CRACM1 (black, n = 5–12) or D110/112A mutant (red, n = 5–14). Currents at −80 mV were assessed at the end of an external application exchange (180 s), set in relation to currents before application (120 s), averaged, and plotted as rest current in percent (%). Data are sorted by application condition (10 mM Ca^{2+}, 10 mM Ba^{2+}, 10 mM Sr^{2+}, 130 mM Na^+, 130 mM K^+, 130 mM Cs^+). Note that monovalent conductances were assessed in nominally Ca^{2+}-free solutions in the presence of standard Mg^{2+} concentrations (2 mM). Data represent the summary of (A) through (H).

remaining Na^+ inward current could then be blocked completely when replacing extracellular Na^+ by TEA^+ (Figure 3B). Additional experiments revealed that the D110/112A mutant also allows limited permeation of K^+ ions, but negligible permeation of Cs^+ in the inward direction (Figure 3D). These results suggest that the aspartate residues in the loop between TM domains 1 and 2 contribute to the selectivity profile of CRACM1 channels, presumably by coordinating Ca^{2+} binding to the outer mouth of the channel and thereby contributing to the discrimination of Ca^{2+} ions against monovalent cations.

On the basis of the above results, one would expect the D110/112A mutant to modify the interplay of divalent and monovalent permeation, which in the wild-type CRAC channel manifests itself in a dose-response curve for extracellular Ca^{2+} with a characteristic anomalous mole-fraction behavior (Figure 3F). Thus, in the complete absence of extracellular divalent ions (nominally divalent-free solution + 10 mM EDTA), CRAC channels allow significant Na^+ permeation. However, exposing cells to just nominally divalent-free solutions without EDTA (free Ca^{2+} and Mg^{2+} estimated at $\sim$1 μM) or adding 10 μM Ca^{2+} virtually eliminates inward currents in wild-type CRACM1 channels (Figure 3E). As Ca^{2+} is increased into the millimolar range, CRAC currents increase again as a result of selective Ca^{2+} permeation. The inhibitory effect of low Ca^{2+} concentrations on Na^+ permeation could be mediated by the binding of Ca^{2+} to the aspartate residues in the first extracellular loop. Indeed, the D110/112A mutant produces significant inward currents even when 10 μM Ca^{2+} is present extracellularly (Figure 3E), changing the anomalous mole-fraction behavior of CRAC channels (Figure 3F). At higher concentrations of Ca^{2+}, the current again behaves similar to the wild-type and becomes Ca^{2+} selective. Finally, we tested whether this mutant also affects selectivity among divalent cations. When extracellular Ca^{2+} is replaced by equimolar Ba^{2+} or Sr^{2+}, wild-type CRACM1 currents are significantly smaller than those carried by Ca^{2+}, amounting to <10% (Figure 3G). Figure 3H shows that the D110/112A mutant produced only marginally increased Ba^{2+} and Sr^{2+} currents, indicating that the mutant largely retains relative selectivity for divalent cations. The bar graph in Figure 3I summarizes the relative magnitude of inward current carried by divalent and monovalent cations in wild-type and D110/112A CRACM1 channels, demonstrating similar divalent permeation, but significantly increased permeation of Na^+ in particular.

The present results, summarized by the hypothetical schematic in Figure 4, would be consistent with a scenario that is analogous to voltage-gated Ca^{2+} channels, in that multiple acidic and negatively charged glutamate and aspartate residues interact to coordinate the binding of Ca^{2+} to the outer mouth of the CRAC channel, thereby providing the molecular basis for its high Ca^{2+} selectivity. This notion would also be consistent with the possible binding of one Ca^{2+} ion in the vicinity of the E106 and E190 residues and a second Ca^{2+} ion that is coordinated by the aspartates in the extracellular loop. Multiple Ca^{2+} binding sites would then be responsible for both discrimination against other cation species and electrostatic repulsion that moves Ca^{2+} ions through the pore in single-file manner. Multiple Ca^{2+}-ion occupancy of the channel could also account, at least in part, for the behavior of outward currents in the mutants. Thus, the occupancy of the wild-type channel pore by two Ca^{2+} ions may present too much of a barrier for the outward movement of cations, whereas partial removal of Ca^{2+} binding sites by the mutant channels may enable significant outward fluxes of monovalent cations.

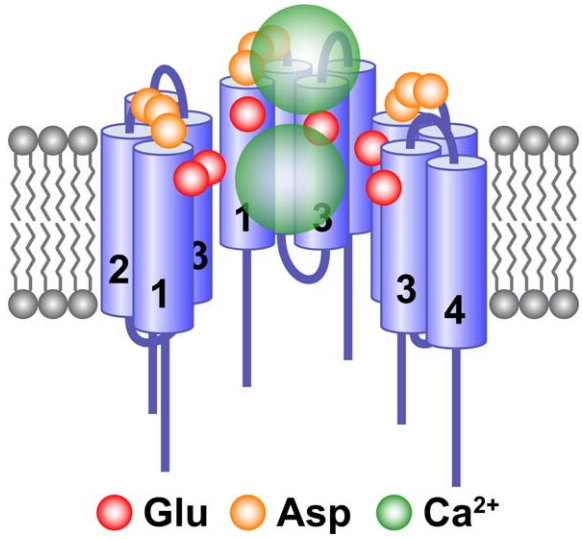

Figure 4. Hypothetical Schematic of CRACM1 Assembly

The schematic summarizes our experimental observations, depicting three CRACM1 molecules within a multimeric assembly, whose exact unit number remains to be established. Because glutamate residues E106 in TM1 and E190 in TM3 affect ion selectivity, both likely face the lumen of the pore. This could be achieved by an N shaped geometry of the four TM domains so that TM domains 1 and 3 become neighbors, each providing slightly asymmetric orientations of glutamate pairs. Together, the multimers can form a ring of negative charges that provides a high-affinity binding site for one Ca^{2+} ion. The aspartate residues in the loop between TM1 and TM2 might create a second high-affinity Ca^{2+} binding site that, when occupied with Ca^{2+}, could provide electrostatic potential for moving the glutamate-bound Ca^{2+} ion through the pore.

Taken together, the results of the present study demonstrate that the CRACM1 protein forms multimeric ion-channel complexes in the plasma membrane, where they can be activated after Ca^{2+} store depletion, presumably by interacting with STIM1. The channel pore of CRACM1 is highly selective for Ca^{2+} ions because of the presence of critical glutamate residues in TM1 and TM3 (E106 and E190) as well as aspartate residues (D110 and D112) within a Ca^{2+} binding motif located in the extracellular loop that connects TM1 and TM2. Mutations of either of these critical residues alter the CRAC-channel selectivity by enhancing monovalent cation permeation relative to Ca^{2+}, providing unambiguous evidence that CRACM1 harbors the CRAC-channel pore.

Supplemental Data

Supplemental Data include Experimental Procedures and are available with this article online at: http://www.current-biology.com/cgi/content/full/16/20/2073/DC1/.

Acknowledgments

We thank M. Bellinger for help with cell culture and M. Koblan-Huberson and K. Troncoso for technical assistance. We have been

supported in part by National Institute of Health grants 5-R37-GM053950 (J.-P.K.) and R01-AI050200 (R.P.).

Received: August 11, 2006
Revised: August 28, 2006
Accepted: August 29, 2006
Published online: September 14, 2006

References

1. Hoth, M., and Penner, R. (1992). Depletion of intracellular calcium stores activates a calcium current in mast cells. Nature *355*, 353–356.
2. Hoth, M., and Penner, R. (1993). Calcium release-activated calcium current in rat mast cells. J. Physiol. *465*, 359–386.
3. Zweifach, A., and Lewis, R.S. (1993). Mitogen-regulated Ca^{2+} current of T lymphocytes is activated by depletion of intracellular Ca^{2+} stores. Proc. Natl. Acad. Sci. USA *90*, 6295–6299.
4. Parekh, A.B., and Penner, R. (1997). Store depletion and calcium influx. Physiol. Rev. *77*, 901–930.
5. Parekh, A.B., and Putney, J.W., Jr. (2005). Store-operated calcium channels. Physiol. Rev. *85*, 757–810.
6. Liou, J., Kim, M.L., Heo, W.D., Jones, J.T., Myers, J.W., Ferrell, J.E., Jr., and Meyer, T. (2005). STIM is a Ca^{2+} sensor essential for Ca^{2+}-store-depletion-triggered Ca^{2+} influx. Curr. Biol. *15*, 1235–1241.
7. Roos, J., DiGregorio, P.J., Yeromin, A.V., Ohlsen, K., Lioudyno, M., Zhang, S., Safrina, O., Kozak, J.A., Wagner, S.L., Cahalan, M.D., et al. (2005). STIM1, an essential and conserved component of store-operated Ca^{2+} channel function. J. Cell Biol. *169*, 435–445.
8. Zhang, S.L., Yu, Y., Roos, J., Kozak, J.A., Deerinck, T.J., Ellisman, M.H., Stauderman, K.A., and Cahalan, M.D. (2005). STIM1 is a Ca^{2+} sensor that activates CRAC channels and migrates from the Ca^{2+} store to the plasma membrane. Nature *437*, 902–905.
9. Feske, S., Gwack, Y., Prakriya, M., Srikanth, S., Puppel, S.H., Tanasa, B., Hogan, P.G., Lewis, R.S., Daly, M., and Rao, A. (2006). A mutation in Orai1 causes immune deficiency by abrogating CRAC channel function. Nature *441*, 179–185.
10. Vig, M., Peinelt, C., Beck, A., Koomoa, D.L., Rabah, D., Koblan-Huberson, M., Kraft, S., Turner, H., Fleig, A., Penner, R., et al. (2006). CRACM1 is a plasma membrane protein essential for store-operated Ca^{2+} entry. Science *312*, 1220–1223.
11. Zhang, S.L., Yeromin, A.V., Zhang, X.H., Yu, Y., Safrina, O., Penna, A., Roos, J., Stauderman, K.A., and Cahalan, M.D. (2006). Genome-wide RNAi screen of Ca^{2+} influx identifies genes that regulate Ca^{2+} release-activated Ca^{2+} channel activity. Proc. Natl. Acad. Sci. USA *103*, 9357–9362.
12. Mercer, J.C., Dehaven, W.I., Smyth, J.T., Wedel, B., Boyles, R.R., Bird, G.S., and Putney, J.W., Jr. (2006). Large store-operated calcium-selective currents due to co-expression of Orai1 or Orai2 with the intracellular calcium sensor, Stim1. J. Biol. Chem. *281*, 24979–24990.
13. Peinelt, C., Vig, M., Koomoa, D.L., Beck, A., Nadler, M.J., Koblan-Huberson, M., Lis, A., Fleig, A., Penner, R., and Kinet, J.P. (2006). Amplification of CRAC current by STIM1 and CRACM1 (Orai1). Nat. Cell Biol. *8*, 771–773.
14. Soboloff, J., Spassova, M.A., Tang, X.D., Hewavitharana, T., Xu, W., and Gill, D.L. (2006). Orai1 and STIM reconstitute store-operated calcium channel function. J. Biol. Chem. *281*, 20661–20665.
15. Spassova, M.A., Soboloff, J., He, L.P., Xu, W., Dziadek, M.A., and Gill, D.L. (2006). STIM1 has a plasma membrane role in the activation of store-operated Ca^{2+} channels. Proc. Natl. Acad. Sci. USA *103*, 4040–4045.
16. Soboloff, J., Spassova, M.A., Hewavitharana, T., He, L.P., Xu, W., Johnstone, L.S., Dziadek, M.A., and Gill, D.L. (2006). STIM2 is an inhibitor of STIM1-mediated store-operated Ca^{2+} entry. Curr. Biol. *16*, 1465–1470.
17. Voets, T., Prenen, J., Fleig, A., Vennekens, R., Watanabe, H., Hoenderop, J.G., Bindels, R.J., Droogmans, G., Penner, R., and Nilius, B. (2001). CaT1 and the calcium-release activated calcium channel manifest distinct pore properties. J. Biol. Chem. *276*, 47767–47770.
18. Tang, S., Mikala, G., Bahinski, A., Yatani, A., Varadi, G., and Schwartz, A. (1993). Molecular localization of ion selectivity sites within the pore of a human L-type cardiac calcium channel. J. Biol. Chem. *268*, 13026–13029.
19. Yang, J., Ellinor, P.T., Sather, W.A., Zhang, J.F., and Tsien, R.W. (1993). Molecular determinants of Ca^{2+} selectivity and ion permeation in L-type Ca^{2+} channels. Nature *366*, 158–161.

Note Added in Proof

After completion of the present study and while this manuscript was under review, two online publications presented data that partially overlap with our findings. Yeromin et al. (2006, *Nature*, 10.1038/nature05108) found that *Drosophila* STIM and Orai coimmunoprecipitate and that the *Drosophila* Orai E180D mutation (corresponding to our human E106D mutant) reduces the selectivity of CRAC currents. Prakriya et al. (2006, *Nature*, 10.1038/nature05122) used the same E106D mutant as we did and arrive at similar conclusions regarding its reduced selectivity. The latter study finds that the E190Q mutation also affects selectivity, in general agreement with our findings. Neither of the studies demonstrates CRACM1 multimerization or identifies the aspartate residues (our D110/112A mutation) as a third site that alters pore selectivity.